DEPÓSITO LEGAL ppi 201502ZU4666
Esta publicación científica en formato digital
es continuidad de la revista impresa
ISSN 0041-8811
DEPÓSITO LEGAL pp 76-654

Revista de la Universidad del Zulia

Fundada en 1947
por el Dr. Jesús Enrique Lossada

Ciencias del Agro Ingeniería y Tecnología

Año 11 N° 29
Enero - Abril 2020
Tercera Época
Maracaibo-Venezuela

(4n +2)π Huckel's rule of $B_n N_n C_{(8-2n)} H_8$ as anti-cancer heterocyclic systems

Neda SamieiSoofi*
Majid Monajjemi**

ABSTRACT

Replacing of Boron and nitrogen atoms in [8] annulene molecule help us for explaining the details of mentioned magnetic mechanism concerning the ring currents of the carbon disappearing in the isoelectronic azabora-hetero-cycles variants ($B_n N_n C_{(8-2n)} H_8^{2-}$,n=0,1,2,3 and4 The (4n+2)π systems aromatic on variants of BnNnC(8-2n) H8 (n=0, 1 ,2,3 and 4) via the localized orbital by considering the current density induced have been studied. It has been predicted a four-electron dia-tropic (aromatic) ring current for (4n+2) π azabora-hetero-cycles variants of BnNnC (8-2n) H8(n=0,1 ,2,4) and a two-electron para-tropic (anti-aromatic) current for (4n) π. HOMO and LUMO energies and also HOMO/LUMO overlapping in whole space have been calculated. Two forms can be considered, first the HOMO–LUMO transition leads to a para-tropic contribution, and second HOMO–LUMO+1 transitions to the dia-tropic contributions. In addition, the NICS and SNICS values confirm the amounts of aromaticity and anti-aromaticity in those rings.

KEYWORDS: Aromaticity, LOL, ELF, Annulene, current density induced, azabora-hetero-cycles.

*Department of Chemistry, Science and Research Branch, Islamic Azad University, Tehran, Iran.
**Department of chemical engineering, Central Tehran Branch, Islamic Azad University, Tehran, Iran. Maj.monajjemi@iauctb.ac.ir

Recibido: 09/01/2020 Aceptado: 12/02/2020

(4n +2) π Regla de Huckel de Bn NnC (8-2n) H8 como sistema heterocíclico contra el cáncer

RESUMEN

El reemplazo de los átomos de boro y nitrógeno en la molécula de anuleno [8] nos ayuda a explicar los detalles del mecanismo magnético con respecto a las corrientes anulares del carbono que desaparecen en las variantes isoelectrónicas de azabora-heterociclos (Bn Nn C (8-2n) H82- , n = 0,1,2,3 y4. Los sistemas (4n + 2) π aromáticos en variantes de BnNnC (8-2n) H8 (n = 0, 1, 2,3 y 4) se ha estudiado la densidad de corriente inducida a través del orbital localizado. Se ha predicho una corriente de anillo dia-trópico (aromático) de cuatro electrones para (4n + 2) π aza-bora-heterociclos variantes de BnNnC (8-2n) H8 (n = 0 , 1, 2,4) y una corriente para-trópica (antiaromática) de dos electrones para (4n) π. las energías HOMO y LUMO y también la superposición de HOMO / LUMO en todo el espacio. Se han calculado dos formas, primero, la transición HOMO-LUMO conduce a una contribución para-trópica, y la segunda transición HOMO-LUMO + 1 a las contribuciones dia-trópicas. Además, los valores NICS y SNICS confirman las cantidades de aromaticidad y anti-aromaticidad en esos anillos.

PALABRAS CLAVE: Aromaticidad, LOL, ELF, Annulene, inducida por densidad de corriente, azabora-heterociclos.

Introduction

1,3,5,7-Cyclooctatetraene (COT) is known as "Annulene" and in contrast of benzene structure, COT follows a nonplanar conformation with alternating double and single bonds via D_2d symmetry (Willstätter and Waser, 1911; Willstätter and Heidelberger, 1913). $C_8H_8^{2-}$, is an aromatic ring with high resonance energy in the aromatic reactions. This molecule is both planar and octagonal in the shape and aromatic with the Huckel electron count of (4×2) +2=10. Huckel's long-standing "4n+2" rule indicates mono aromatic rings from anti-aromatics, and correlates the electronic structures of those systems with their magnetic properties (Gellini and Salvi, 2010). Through the interaction between alternating bonds it has been confirmed that the structure of COT involves a planar transition state of D_{4h} symmetry (Wu et al., 2012). Moreover the NMR experimental data indicate that COT^{2-} also adopts a D_{8h} symmetry structure (Naor and

Luz, 1982). Although the planar D_{4h} structure for the ring inversion of COT has a transition state (TS) with around 12 kcalmole^{-1} barrier energy (Nishinaga et al., 2010), the D_{8h} bond switching TS lays a few kilo calories per mole higher. Actually, COT has three fundamental structural changing including 1- ring inversion, 2-bond shifting and 3- valence isomerization (Schild and Paulus, 2013).

Planar conjugated COT^{2-} exhibit a strong link between p-electrons. Coupling between COT^{2-} charge state and its mechanical conformation creates new opportunities for COT^{2-} as an aromatic molecule including electromechanical converter treatment (Wenthold et al., 1996).

Replacing of Boron and nitrogen atoms in COT help us for explaining the details of mentioned magnetic mechanism concerning the ring currents of the carbon disappearing in the isoelectronic azabora-hetero-cycles variants ($B_nN_nC_{(8-2n)}H_8^{2-}$,n=0,1,2,3and4 scheme.1 (Wu et al., 2012) and (Stevenson et al., 1998) . Steiner and coworkers investigated a model via frontier-orbital contributions which yields an accurate account of p ring currents in benzene, COT^{2-} and suchlike planar rings (Schild and Paulus, 2013). London, Pauling and Pople investigated the concept of aromaticity and anti-aromaticity in view point of magnetic criterion, diatropic (Planer of 4n+2 systems) and paratropic currents (planar of 4n systems) (Yoshida et al., 2015). Recently, it has been shown that the ring currents are a consequence of the HOMO–LUMO transition depends on symmetry properties (Andrés et al., 1998). For the 4n+2 hetero-cycles, $B_nN_nC_{(8-2n)}H_8^{2-}$(n=0,2,4), densities maps, exhibit the "p" electrons with the localized circulations around the electronegative nucleus (Hrovat and Borden, 1992).

In this work we exhibited that an extension of the figurative orbital model is able to account for both the currents in carbocyclic aromatic rings and their B-N analogues such as $B_4N_4H_8^{2-}$. Although it is generally agreed that $B_3N_3H_6$ is not aromatic (due to localized of p electrons on the more negative nitrogen atoms), they have suitable resonance energies for aromatic reactions. Although a few derivatives of the homologues rings of $B_nN_nC_xH_y$ such as diazadiboretane and borazoin have been synthesized, some compounds

of $B_nN_nC_{(8-2n)}$ H_8^{2-} (n=0,2,4) have not been prepared yet. Therefore any theoretical calculation and detailed discussion might be useful for understanding in the area of aromaticity and also physical chemistry mechanism of these kind compounds.

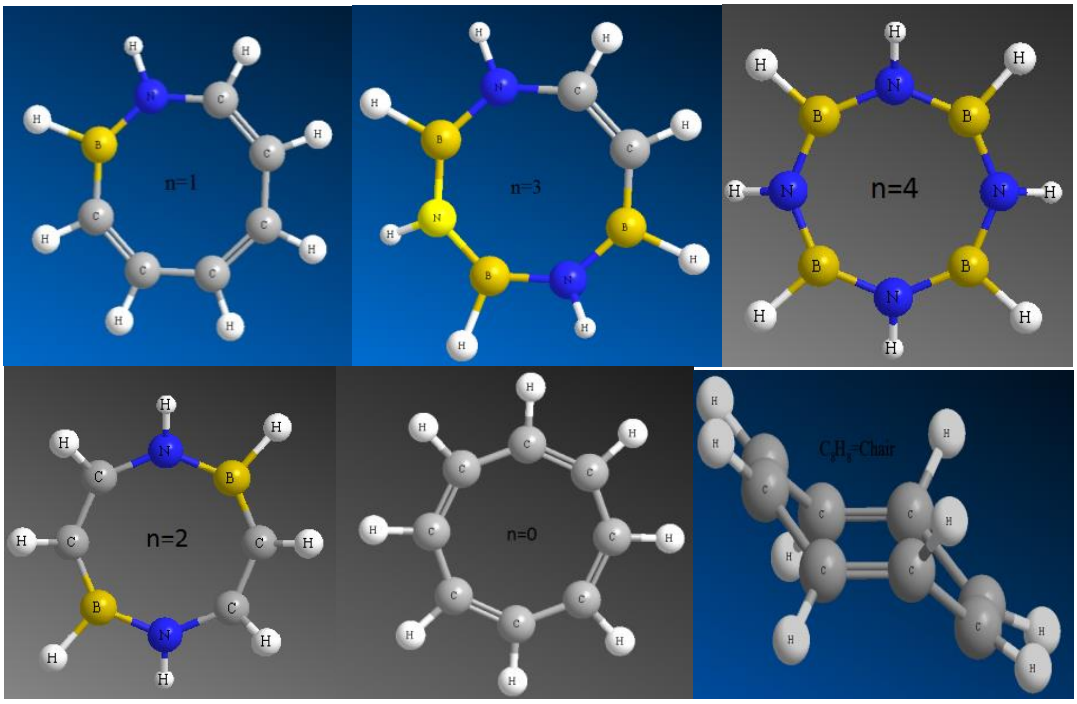

Scheme.1: $B_n N_n C_{(8-2n)} H_8$, including n=0 ,1, 2,3 and 4

1. Theoretical background

1-1. Aromaticity & ring current

Current-density's map can be estimated through theoretical methods without any gauge-dependence problem by vector potential generating of the magnetic field. Meanwhile from occupied to unoccupied orbitals, the total current densities are evaluated which are modulated and governed by energy denominators and symmetry rules respectively. Aromaticity can be also defined through magnetic criteria (Longuet, 1967) and is a trustworthy account of the currents induced by an external magnetic field capability. In addition chemical shift, isotropy, anisotropy, span, asymmetry and other properties are all integrals of these current densities . For the magnetic criterion, the

resultant of all such components explains the aromaticity or anti-aromaticity which is related to the net dia-tropicity and para-tropicity of the ring current respectively.

1.2. Anticancer properties, heterocyclic rings and Aromaticity

Cancer is one of the important causes of death in the new century. This work is done for developing of modern anticancer drugs. Many of heterocyclic compounds are known as anticancer drugs such as alkylating agents which have targeted cell DNA causing cell death. Heterocyclic structures are composed by atoms other than carbon, where the most times substituents are sulfur, oxygen, Boron and nitrogen. The model size of heterocyclic ring such as $B_n N_n C_{(8-2n)} H_8$, with the substituent group of the core scaffold, impact tightly on the chemical and physical properties while among the clinical applications, heterocyclic compound has an active role as anti-bacterial, anti-viral , anti-fungal , anti-inflammatory and anti-tumor drugs. Traditional drugs for anticancer such as alkylating agent has targeted cell DNA causing cell death. Generally, chemical-physics and biochemical properties like donor-acceptor capability, hydrogen bond, π-π stacking interactions, van der Waals, co-ordination bonds with metals and in total hydrophobic forces have caused the increasing interest in anticancer studies for such compounds $B_n N_n C_{(8-2n)} H_8$. These properties are important of understanding for their reactivity enable derivatives to readily bind with various nucleic acids, enzymes and biological structures.

1.3. Isotropic and anisotropic parameter

Spherical tensors can be noted as $\sigma_0^{iso(2)} = \sqrt[2]{3/2}\,\zeta_{(zz)}$ And $\sigma_{\pm 2}^{sym(2)} = \frac{1}{2}\zeta_{(zz)}$ **(1)**

Where, $\zeta_{(zz)}$ is the reduced anisotropy and can be calculated through $[\zeta_{(zz)} = (\sigma_{zz} - \sigma_{iso}) = (\sigma_{33} - \sigma_{iso})]$**(2)**. Haeberlen and Mehring (Haeberlen, 1967) have investigated fundamental tensors as $\sigma = \sigma^{iso(0)} + \sigma^{anti(1)} + \sigma^{sym(2)}$ **(3)**. This parameter is related to the anisotropy $(\Delta\sigma)$ with $\Delta\sigma = \frac{3}{2}\zeta_{(zz)}$ **(4)** and (η) shielding which can be estimated via

:$\Delta\sigma = \sigma_{zz} - \frac{1}{2}(\sigma_{xx} + \sigma_{yy})$ **(5)** *and* $\eta = \left(\frac{\sigma_{yy}-\sigma_{xx}}{\zeta_{(zz)}}\right) = \frac{3(\sigma_{yy}-\sigma_{xx})}{2\Delta\sigma}$ **(6)** (Anet and O'Leary, 1992).

Since the magnetic resonance of a spin is seldom isotropic, therefore they have to represent by new tensors by Herzfeld-Berger notation. These tensors are known as Span (Ω) Ω ≥ 0, which describes the maximum width of the model and the skew (**κ**) of the tensor which is a magnitude of the values (Ω) $= \sigma_{33} - \sigma_{11}$ **(7)** *and* $\kappa = \frac{3(\sigma_{iso}-\sigma_{22})}{\Omega}$ **(8)**. Moreover the orientation of asymmetry tensor is given by $\kappa = \frac{-3\Upsilon_{(yy)}}{\Omega}$ *or* $\kappa = \frac{3(\sigma_{1so}-\sigma_{22})}{\Omega}$ **(9)** (-1≤ κ ≤ +1), and$\Upsilon_{(yy)} = \sigma_{22} - \sigma_{iso}$. Asymmetry (η) indicates that how much deviation can be appeared from an axially symmetric tensor, therefore the region of η is between zero and one (0 ≤ η ≤ +1) and in some cases η = 0.

1.4. ELF and LOL functions

Electron density can be written as $\rho(r) = \eta_i \left|\varphi_i(r)\right|^2 = \sum_i \eta_i \left|\sum_l C_{l,i}\,\chi_i(r)\right|^2$**(10)**. Where "χ" is the basis function of orbitals and η_i is occupation number. *C* is also a coefficient matrix. The unit of electron density in atomic scale is e/Bohr^3. Bader exhibited that the regions with having large electron localization must have a large magnitude of Fermi-hole integration. Becke and Edgecombe cleared that spherically averaged like-spin pair has direct correlation to the Fermi hole. Consequently, they introduced a new function as "electron localization function" (ELF) (Lu and Chen, 2012).

ELF(r) = $\frac{1}{1+[D(r)/D_{0(r)}]^2}$ **(11)** where

D(r) = $\frac{1}{2}\sum_i \eta_i \left|\nabla\varphi_i\right|^2 - \frac{1}{8}[\frac{\left|\nabla\rho_\alpha\right|^2}{\rho_\alpha(r)} + \frac{\left|\nabla\rho_\beta\right|^2}{\beta(r)}]$ **(12)** and $D_{0(r)} = \frac{3}{10}(6\pi^2)^{\frac{2}{3}}[\rho_\alpha(r)^{\frac{5}{3}} + \rho_\beta(r)^{\frac{5}{3}}]$ **(13)** for close-shell system, since $\rho_\alpha(r) = \rho_\beta(r) = \frac{1}{2}\rho$, *D* and D_0 terms can be simplified as D(r) = $\frac{1}{2}\sum_i \eta_i \left|\nabla\varphi_i\right|^2 - \frac{1}{8}\left[\frac{\left|\nabla\rho\right|^2}{\rho(r)}\right]$ **(14)** and $D_{0(r)} = \frac{3}{10}(3\pi^2)^{\frac{2}{3}}\rho(r)^{\frac{5}{3}}$ **(15)** .

Savin *et al.*, indicated which $D(\mathbf{r})$ reveals the excess kinetic energies densities caused by Pauli repulsion, while $D_0(\mathbf{r})$ can be noted as Thomas-Fermi kinetic energies densities. In other words they reinterpreted ELF in view point of kinetic energy through Kohn-Sham DFT's wave-function. Therefore ELF would be in the range of [0, 1] and a large ELF value indicates that electrons are strongly localized. ELF has been widely used for a wide variety of systems, such as organic and inorganic small molecules, atomic crystals, coordination compounds, clusters.

LOL or Localized orbital locator is another function for locating high localization regions likewise ELF, invistegated by Schmider and Becke. $LOL(r) = \frac{\tau(r)}{1+\tau(r)}$, where $(r) = \frac{D_0(r)}{\frac{1}{2}\sum_i \eta_i \ |\nabla \varphi_i|^{\ 2}}$, (16) $D_0(r)$ for spin-polarized system and close-shell system are defined in the same way as in ELF. LOL has similar expression compared to ELF. Actually, the chemically significant regions that highlighted by LOL and ELF are generally qualitative comparable, while Jacobsen pointed out that LOL conveys more decisive and clearer picture than ELF. Obviously LOL can be interpreted in kinetic energy way as for ELF; however LOL can also be interpreted in view of localized orbital. Small (large) LOL value usually appears in boundary (inner) region of localized orbitals because the gradient of orbital wave-function is large (small) in this area. The value range of LOL is identical to ELF, namely [0, 1].

2. Computational details

Geometry & electronics structures have been accomplished using the m06 groups in (DFT) functional. This methods are based on an iterative solution of Kohn-Sham equation (Kohn and Sham, 1965) of DFT in the plane-waves with the projector-augmented wave pseudo-potentials. The Perdew-Burke-Ernzerhof (PBE) (Perdew et al, 1996) exchange-correlation functional of the generalized gradient approximation (GGA) is adopted. The geometry of each part of ions was optimized at the various methods including M062x/cc-pvdz, M062x/cc-pvtz and CASSCF methods. For obtaining ab-initio amounts on the currents in BN analogues of the 4n and 4n+2 carbo-cycles, calculations

were performed for $C_8H_8^{2-}$, BNC6H8, $B_2N_2C_4H_8$ and $B_4N_4H_8$ and currents were calculated by using the ipsocentric approach. At this level of theory, C_8H_8 and $B_4N_4H_8$ have planar structures with D_{4h} symmetry. To draw the contour line maps of Current-density for both the constrained planar and the fully optimized structures Multiwfn software have been used. We have plotted the contour line corresponding to electron densities=0.001 a.u., which are defined by R. F. W Bader (Bader, 1990). This is useful for analyzing distribution of the electrostatic potential on potential surfaces. Such contour lines have also been plotted in gradient lines and vector field's maps through the same options.

The relief maps were used for presenting the height data at each point. If these values are too large, they will also be truncated in those graphs. Therefore, it can be chosen for scaling the values with a factor for avoiding truncation. Shaded surfaces maps with and without projection are used in our representation of height values at each situation. For confirmation the data several extra calculation including MP4 (SDQ)/6-31+G(d'), QCISD(T)/6-31+G(d') and CAM-b3lyp/6-311g have also been done. The charges transfers were also evaluated using the Merz-Kollman-Singh, chelp, or chelpG . Those methods are based on molecular electrostatic potential approaches (MESP) fitting which are suitable for small molecules (in large molecules some of the innermost atoms are located far away from the points at which the MESP is computed). Obviously the representative atomic charges for molecules should be computed as average values over several molecular conformations. A detailed overview of the effects of the basis set and the Hamiltonian on the charge distribution can be found in.

The electron densities (Both of Gradient and Laplacian), values of orbitals and LUMO, HOMO wave-functions, electrons spin densities, electrostatic potentials from nuclear atomic charges, electrons localization functions (ELF), localized orbital locator (LOL) and total electrostatic potential (ESP), as well as the exchange-correlation densities, correlation holes and correlation factors, and the averages local ionization energies using the Multifunctional Wave-function Analyzer have also been calculated in this work. Among the various methods and basis sets (both large and medium) which have

been used in this study, the cc-pvdz and cc-pvtz basis sets exhibit the most favorable results for electrostatic potential (ESP) fitting. The cc-pvdz is a double-ζ basis set with a single set of polarization functions for B to F and cc-pvtz is a triple-ζ basis set including diffuse functions, double d-polarizations, and a single set of polarization functions. The active space for the CASSCF method was composed of all valence electrons and orbitals of B, N and C atoms. A Quadratic CI calculation including single and double substitutions has been used to evaluate various one-electron properties including NBO, bonding analysis, atoms in molecules (AIM), natural population analysis, multipole moment, electrostatic potentials, and electrostatic potential-derived charge using the Merz-Kollman-Singh, chelp, or chelpG (Besler et al., 1990).

The AIM keyword is also used for computing the atomic charges of atoms in molecules, covalent bonds, localized orbitals, and critical points for any further properties predication of atoms in molecules (Chirlian and Francl, 1987). In addition Polarizabilities and hyper-polarizabilities have been calculated through CISD, QCISD and CASSCF methods. CHELPG charges (Martin and Zipse, 2005) can also be computed using the well-known ab initio quantum chemical packages such as Gaussian or GAMESS-US. In this study, it is indeed difficult and at some points not important to use the large basis sets and demanding methods such as MRCI for CHELPG and ESP calculations due to the large number of calculations in various situations of MESP simulation. Therefore, with medium methods in terms of computational cost, we have found the accurate results for our approach. All the calculations were performed using the Gaussian program package and the optimization were done along with the frequencies calculation for confirming that the geometries were real minimum without any imaginary frequencies.

3. Result and discussion

The compounds of $B_n N_n C_{(8-2n)} H_8$, (n=1,2,3 and 4) have not been synthesized, although many derivatives of the homologues such as di-aza-di-boretidine and borazocine have been prepared.

Although 8p-electron of $B_nN_nC_{(8-2n)}H_8$, (n=2,4) were originally called "an inorganic Compounds" and believed to have a resonance energy similar to that of Annulene, they were soon recognized that they took part in few reactions typical of aromatic systems. Geometries and energies of $C_8H_8^{2-}$ in various methods have been listed in Table.1. It has been exhibited(Table.1) that m062x/cc-pvTz method has more accurate results compare to other methods, therefor this method has been considered for investigation and calculation on variant of $B_n N_n C_{(8-2n)} H_8$, (n=0 ,1,2,3 and 4). It is now generally agreed that homologues rings of $B_nN_nC_xH_y$ such as diazadiboretane and borazoin are not aromatic.

In contrast to benzene or $C_8H_8^{2-}$, the p electrons are localized on the more negative nitrogen atoms, even if a few chemical behaviors are reminiscent of that of aromatic rings. ELF current-density map from ab initio calculations on COT^{-2} and $B_4N_4H_8^{2-}$, are shown in (Fig.1) and the currents are dominated by HOMO contributions Table 2.

Table.1: Geometry and energy of $C_8H_8^{2-}$ in various methods

Methods	Energy (Hartree)	C-C &C-H in resonated ring (Å)
MP4(SDQ)/6-31+G(d')	-308.46562	1.415, 1.100
QCISD(T)/6-31+G(d')	-308.52139	1.415, 1.08
CAM-b3lyp/6-311g	-309.24996	1.413, 1.099
m062x/cc-pvdz	-309.33567	1.415, 1.05
m062x/cc-pvTz	-309.43505	1.409, 1.094

Table.1: continue: HOMO/LUMO and Aromaticities

C-C-C and H-C-C angle in resonated ring	LUMO/HOMO Gap Energy $kJmol^{-1}$	Aromaticity	
		NICS	S-NICS
135.0, 112.5	519.06	-14.95	-15.85
135.0, 112.5	519.13	-15.11	-15.83
135.0, 112.5	519.05	-14.87	-15.87
135.0, 112.5	547.1	-17.59	-15.88
135.0, 112.5	493.43	-15.90	-15.82

Table 2. HOMO/LUMO and Aromaticities

Molecule	LUMO/ HOMO Gap energy	% composit for HOMO	% composition of atoms for LUMO
$B_4N_4H_8^{2+}$	3.34 eV	23.0(B1+B4 +B6+B7)	7.8 (B1+ B4 + B6 + B7) +10.5 (N2+N3+N5+N8)
$B_4N_4H_8^{2-}$	3.54 eV	25.0(B1+B4 +B6+B7)	6.8 (B1+ B4 + B6 + B7) + 11.5 (N2+N3+N5+N8)
$B_4N_4H_8^{0}$	3.14 eV	26.0(B1+B4 +B6+B7)	7.1 (B1+ B4 + B6 + B7) + 12.1 (N2+N3+N5+N8)
$B_2N_2C_4H_8^{2-}$	4.055 eV	30.0(B1+B7) + 4.0 C3+ C5) + 15.9 (C4+C6)	9.0 (B1+B7)+ 19.4 (N2+N8)- 4.7(C3+C5) + 34.6(C4+C6)+9.1B7
$BNC_6H_8^{2-}$	4.59 eV	7.0N1+8.6B2 +1.2C3+23.0 (C4+C8)+0. 6C5+33.4C 6+0.9C7	1242B2-43N1-1580C3+99 C4+4205C5+5610C6+15 207 C7

In a ring with "4n+2" electrons, the HOMO and LUMO are related to "n+1" and "n", but for a ring with "4n" electrons, the HOMO and LUMO are derived from a split degenerate (λ=n). For n=4 or $B_4N_4H_8$ λ is zero and meanwhile dia-tropic contribution arises from a transition in which $\Delta\lambda$ =+1 and a para-tropic contribution arises from a transition in which $\Delta\lambda$ =0 .

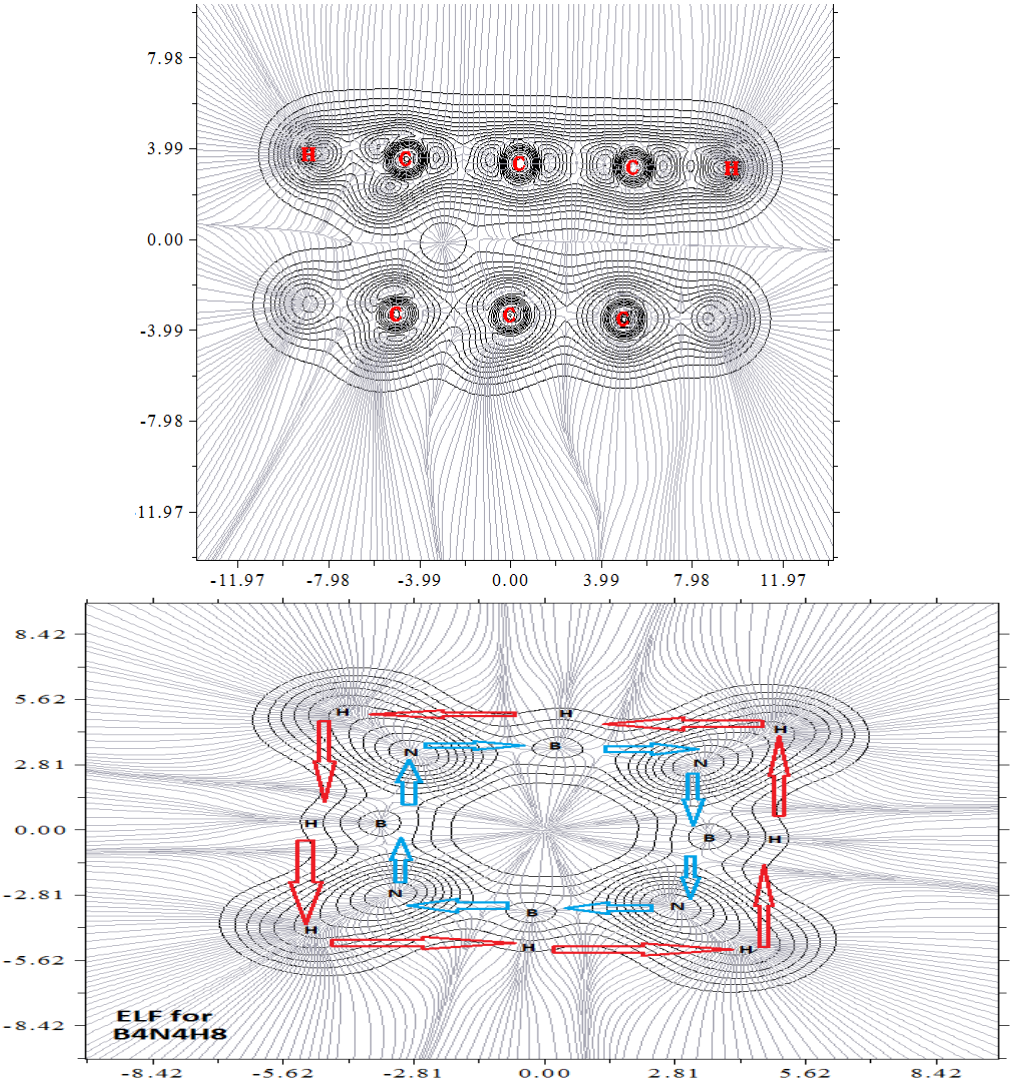

Fig1: Gradient lines map of ELF and current density induced in cyclooctatetraene ($C_8H_8^{2-}$) and boron nitride in cyclooctatetraene ($B_4N_4H_8^{2-}$) by a perpendicular external magnetic field.

Calculated by the Cam-B3lyp/ 6-31G**. Anticlockwise circulations are Dia-tropic, clockwise circulations Para-tropic

% composition of atoms for (HOMO-1)	HOMO/LUMO overlap in whole space	HOMO/HOMO -1 overlap	Molecule
23(N2+N3+N5+N8)	0.314	0.323	$B_4N_4H_8^{2+}$
25(N2+N3+N5+N8)	0.348	0.338	$B_4N_4H_8^{2-}$
26(N2+N3+N5+N8)	0.316	0.344	$B_4N_4H_8^{0}$
0.02B1+15.3N2+28.9C3+5.7 C4+28.8C5+5.7C6+0.01B7+ 15.3N8	0.333	0,554	$B_2N_2C_4H_8^{2-}$
13.4N1+1.1B2+2.5C3+21.3C 4+16.8C5+0.5C6+23.7C7+1 5.4C8	0.152	0.718	$BNC_6H_8^{2-}$

Therefore for the 4n+2 systems (with higher symmetry) only the HOMO–LUMO transitions are consider (dia-tropic current) and for the "4n" ring (lower symmetry) two forms can be considered , first the HOMO–LUMO transition leads to a para-tropic contribution, and second HOMO–LUMO+1 transitions to the dia-tropic contributions (Table.2)(Monajjemi et al, 2010; Monajjemi and Khaleghian, 2011; Monajjemi, 2012). In Huckel theory it is needed to rearrange the Coulomb and resonance integral parameters as: (1) boron and nitrogen are zero- and two- electron.

Table.3: HOMO and LUMO characteristics in several molecules

Therefore in structure of $B_nN_nH_n$ with the differing electro-negativities of boron and nitrogen a symmetric changing to the Coulomb parameters yield $(\alpha-\gamma\beta)$ and $(\alpha+\gamma\beta)$ energies which γ is a correlated parameter in various $B_nN_nH_n$ structures and varied between $0\leq\gamma<1$. Solution of the Huckel equation via considering the γ parameter with a simple modification gives molecular orbitals $\{\emptyset\}$ and related energies $\{\varepsilon\}$ from which the Consequences for cycle currents can be deduced. Canonical molecular orbitals (Streitwieser, 1961) $(\Psi_{\lambda,c})$ are delocalised set with $(\gamma=0)$ and in each position of $\gamma\neq0$ a linear combinations of these set can be written for orbitals.

In the full symmetrical systems of carbocyclic, the degeneracy of $\Psi_{2,c}$ and $\Psi_{2,s}$ can be stabilized through several ways such as distortion to D_2d and D4h geometries of "clamped"-substituted COT systems. Due to its bond alternation, planar D4h COT keeps delocalized orbitals and the cycle current of the equilateral carbocyclic, as Fig.1 exhibits. In the heterocyclic systems or $(\gamma\neq0)$ $\Psi_{2,c}$ and $\Psi_{2,s}$ are bonding and antibonding wave function, respectively, and are belongs to the B1u and B2u symmetric on the setting of D4h within D8h. It is notable wave functions $\Psi_{2,c}$ and$\Psi_{2,s}$, is the HOMO and LUMO, for all amounts of γ, which is completely localized, the HOMO on the nitrogen atom and the LUMO on the boron atom. Obviously,$\emptyset_{0,c}$, $\emptyset_{1,c}$, $\emptyset_{1,s}$, $\emptyset_{3,c}$,$\emptyset_{3,s}$ and $\emptyset_{4,c}$, become strongly localized on the electronegative atom. In the $\gamma=1$ the nitrogen and boron atoms Obey from Huckel's population as $1\pm\frac{1}{2}(\frac{1}{2}+\frac{1}{\sqrt{3}}+\frac{1}{2\sqrt{5}})\approx 1.66$ and 0.36 electrons, respectively. In the Huckel–London approach the ring current of the eight-membered ring in small amount of γ, HOMO–LUMO contribution overcome to the bond–bond polarizability. By increasing the γ from the planar-constrained of COT (where $\gamma=0$) to the B4N4H8 planer (where $\gamma=1$), the eight-membered ring has still net para-tropic circulation. The symmetry conclusion to deduct the line currents in 4n π position includes several steps; firstly $(\gamma\approx0)$, those currents are overmatched via the HOMO–LUMO transitions amongst small gap energies. This situation $(\Delta\lambda=0)$ generates an intense, para-tropic intensities.

In other words the symmetry reasoning for deducing the currents in 4n systems consist of several levels from (γ =0), which the current is under HOMO–LUMO transition with a small energy gap towards γ =1which, the HOMO–LUMO gap opens, and the intensity of the current falls but remains paramagnetic. Here the separation of HOMO-1 and LUMO as well as HOMO and LUMO+1 increase slowly and the para-tropic or anti-aromatic cycle current is reduced Significantly.(Tables2-4), Current-density maps, ELF and LOL from ab-initio calculations on the $B_nN_nC_{(8-2n)}H_8^{2-}$, are shown in Figures1-3 and are listed in tables 4,5.

Aromatic fluctuation index (FLU) & De-localization index (DI)	Para delocalization index(PDI)	Para linear response indexes (PLR)	Molecule
FLU=0.002 DI for all B-N atoms pair in the ring =1.24	PDI=0.041	PLR=0.18	$B_4N_4H_8^0$
FLU=0.001 DI for all B-N atoms pair in the ring =1.30	PDI=0.031	PLR=0.16	$B_4N_4H_8^{2-}$
FLU=0.000 DI for all atoms pair in the ring =1.46	PDI=0.035	PLR=0.14	$B_3N_3C_2H_8^{2-}$
FLU=0.003 DI for B1-N2 atom pair= 1.370 and for N2-C4=1.4 And for C4-C5=1.6	PDI=0.029	PLR=0.15	$B_2N_2C_4H_8^{(0)}$
FLU=0.003 DI for N1-B2 =1.32	PDI=0.014	PLR=0.04	$BNC_6H_8^{2+}$

Table.4, 5: continue Localization index (LI), Ring perimeter, Aromatic fluctuation, PDI and PLR for variants of $B_n N_n C_{(8-2n)} H_8$, (n=0 ,1,2,3 and4)

Molecule	Ring perimeter(Å) & area(Å^2)	No. Pi Orbitals & No. Pi electrons	Localization index (LI)
$B_4N_4H_8^0$	11.41& 10.12	20 & 10	For all B atoms=3.24 For all N atoms=5.44
$B_4N_4H_8^{2-}$	11.56 & 10.04	22 & 10	For all B atoms=3.195 For all N atoms=5.567
$B_3N_3C_2H_8^{2-}$	11.41 & 9.73	24 & 8	B1 to B3=4.102 N1toN3=3.22 All H atoms=0.345
$B_2N_2C_4H_8^{(0)}$	11.40 & 9.94	16 & 10	B1,B7=3.27 & H9, H15=0.49 N2,N8=5.4
$BNC_6H_8^{2+}$	11.42& 9.84	8&8	N1=5.45, B2= 3.13, C3=4.4, C4=4.33, C5=4.137, C6=4.412, C7=4.5,C8=4.33,

For each molecule, the maps indicate total p and s contributions for inducing current densities. As expected, the currents arising from the p electrons are, respectively, strongly dia-tropic in benzene and strongly para-tropic in COT. The currents are dominated by HOMO contributions in both cases. An angular-momentum analysis shows how the symmetry rules account for these features. At each successive energy level, the

quantum (Daudel et al., 1959) number, l (=0,1...,N/2), increases by one. In a cycle with N=4n+2 electrons, the HOMO and LUMO correspond to l=n and n+1, respectively. It is notable that that photo-excited cyclooctatetraene relaxes toward the planar *D8h*-symmetric and its structure appears to be identical to the thermal double bond shift transition state. This is the typical π-delocalized structure expected to characterize for a Huckel anti-aromatic [4*n*] system. As it can be seen in the Table.3 the some electrons are localized and some other is not on the aza-bora-hetero-cycles variants. For benzene the low energies may only involve one delocalized allyl radical and three adjacent unpaired electrons while , in cyclooctatetraene, due to its larger size, a new and more stable tetra-radical-type configuration might be possible.

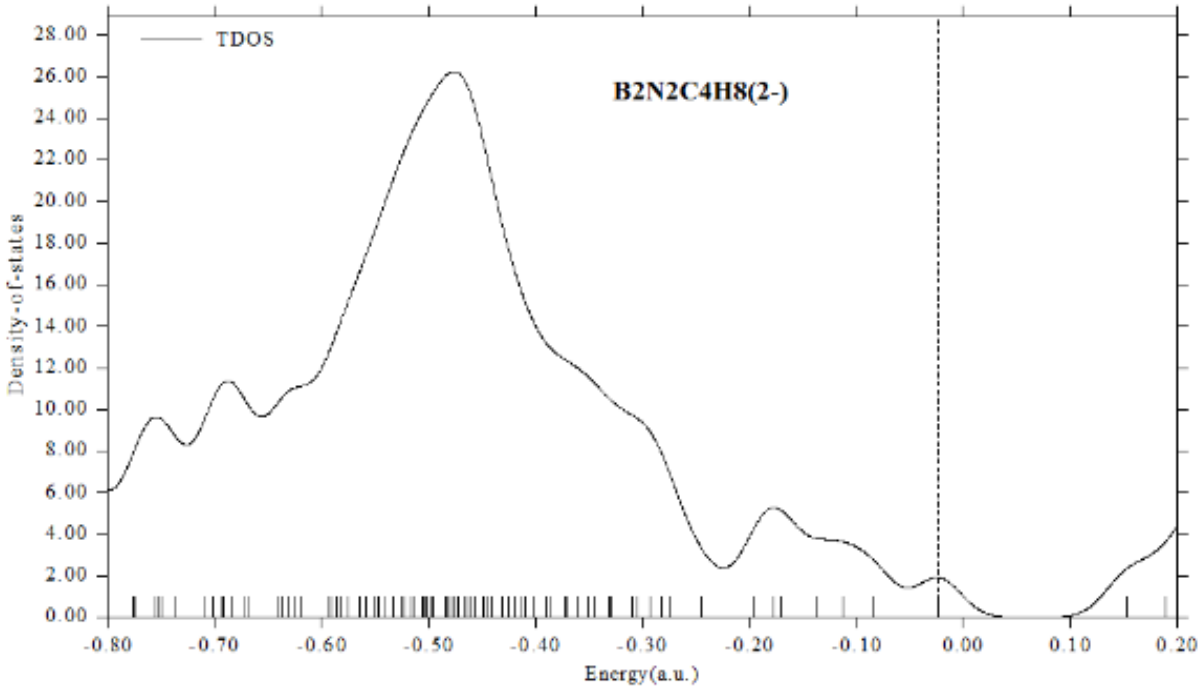

Fig.2: Density of states for π electrons in the rings

Table.5: Various calculations of charges for $C_8H_8^{2-}$ and $B_4N_4H_8^{2-}$

(MK)Merz-Kollman ESP fitting Sum of values=-2	Mayer's valance	Wiberg's bond order
-0.868949, -0.154367 0.430606, 0.092885 0.428573, 0.094883 -0.866058, -0.155198 0.421720, 0.094818 -0.868144, -0.154232 -0.851509, -0.160690 0.417617, 0.098044	3.35, 0.86 2.98, 0.90 2.98, 0.90 3.35, 0.86 2.98, 0.90 3.35, 0.86 3.35, 0.86 2.98, 0.90	B1-N2: 1.244 B1-N3: 1.244 N2-B4: 1.244 B4-N5: 1.244 N5-B7: 1.244 B7-N8: 1.244 N8-B6: 1.244 B6-N3: 1.244

Fig.3: ELF for variants of $B_n N_n C_{(8-2n)} H_8$, (n=0,1 ,2,3 and4)

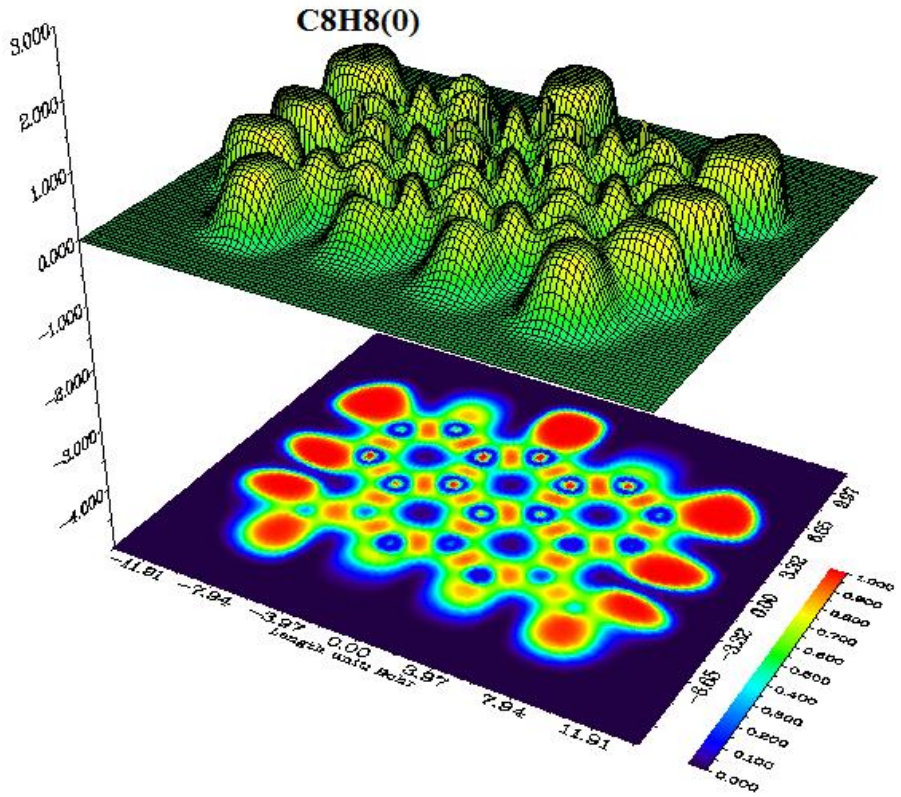

COTs have extended delocalized structures (i.e., identical 1.40 Å π-bonds and planarity, recalling an aromatics system). Therefore, it can be image that COT as being

stabilized by a kind of aromatic effects which plays against the out-of-plane deformation needed for reaching both the boat and the kink structures due to those motions which break delocalization. The total electrostatic potential for variants of $B_nN_n C_{(8-2n)} H_8$, (n=0 ,1,2,4) are plotted in Fig.4. As it can be seen in the Fig.4 the stable electro static for those variant are started in positions 1.40 Å, 1.45 Å, 1.48 Å,1.50 Å for CH_8H_8, $B_4N_4H_8$, $B_2N_2C_4H_8$ and BNC_6H_8 which is correspond to bond length and they will be ended in the positions around 5.5 for CH_8H_8 and 10.5 for other variants.

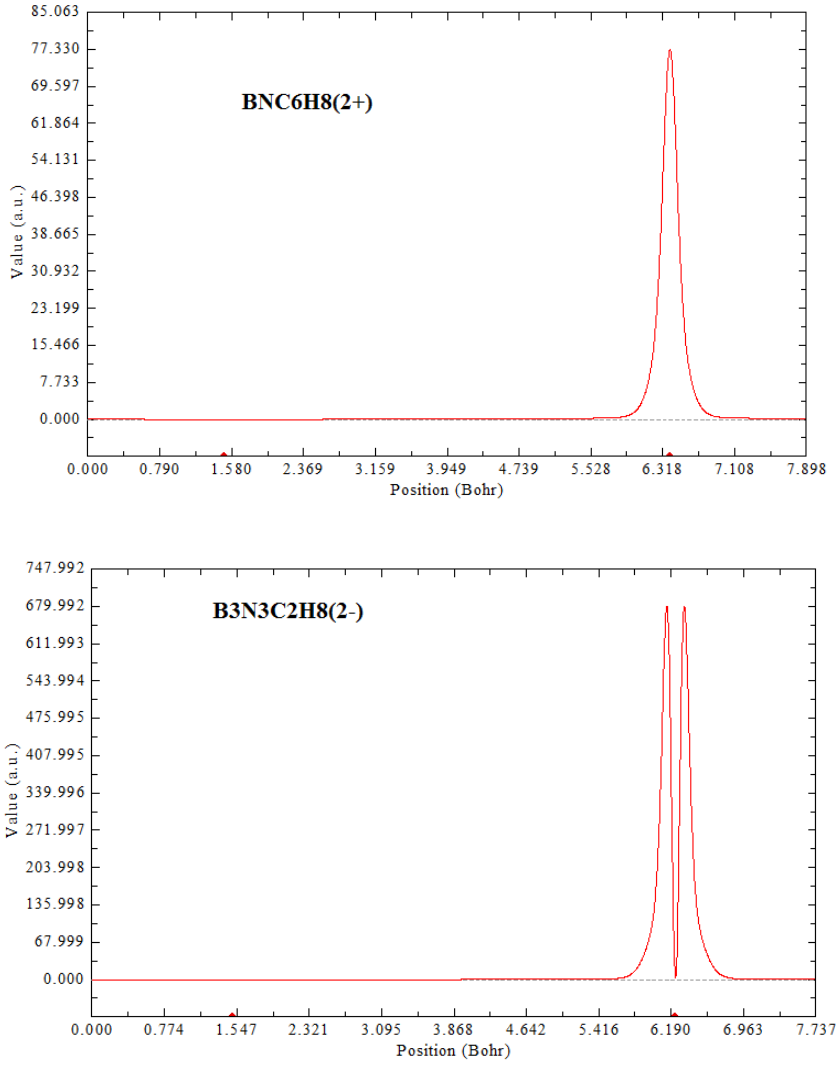

Fig4: Total electrostatic potential for variants of $B_n N_n C_{(8-2n)} H_8$, (n=0,1 ,2,and 4)

Conclusion

Current-density maps, ELF and LOL from ab-initio calculations on the $B_nN_nC_{(8-2n)}H_8^{2-}$, are investigated as a novel method for understanding the aromaticity and anti-aromaticity in heterocyclic compounds by this work. For each molecule, the maps indicate total p and s contributions for inducing current densities. As expected, the currents arising from the p electrons are, respectively, strongly dia-tropic in benzene and strongly para-tropic in COT. The currents are dominated by HOMO contributions in both cases. An angular-momentum analysis shows how the symmetry rules account for these features.

Acknowledgment

We are thankful to IAU University for supporting this work and providing the main equipment and mini computing lab for us.

References

Andrés, J.L., Castaño, O., Morreale, A., Palmeiro, R., Gomperts, R (1998). Potential energy surface of cyclooctatetraene. J Chem Phys 108, 203–207.

Anet, F.A.L., O'Leary, D.G., (1992). The shielding tensor. Part II: Concepts Magn. Reson. 4, 35

Bader, R.F.W. (1990). Atoms in Molecule: A quantum Theory (Oxford Univ. press, Oxford.

Besler, B.H., Merz, K.M., Kollman, P.A (1990). Atomic charges derived from semi empirical methods J. comp. Chem (11): 431-439, DOI: 10.1002/jcc.540110404

Chirlian, L.E., Francl, M.M (1987). Atomic charges derived from electrostatic potentials: A Detailed study. J.comp.chem (8): 894-905, DOI: 10.1002/jcc.540080616

Daudel, R., Lefebvre, R., Moser, C., (1959). Quantum Chemistry, Methods and Applications, Wiley-Interscience, New York, p. 449.

Gellini, C., Salvi, P. R. (2010). Structures of Annulenes and Model Annulene Systems in the Ground and Lowest Excited States. Symmetry 2, 1846–1924.

Hrovat, D.A., Borden, W.T (1992). CASSCF calculations find that D8h geometry is the transition state for double bond shifting in cyclooctatetraene. J Am Chem Soc 114: 5879–5881.

Haeberlen, U. (1976). In Advances in Magnetic Resonance, Suppl. 1 Academic Press, New York. M. Mehring. M, Principles of High Resolution NMR in Solids, 2nd.ed, Springer Verlag, Berlin,

Kohn, W., Sham, L.J. (1965). Self-Consistent Equations Including Exchange and Correlation Effects. Phys. Rev (140) A: 1133-1138

Longuet-Higgins, H.C., (1967). in Aromaticity, Special Publication No. 21, The Chemical Society, London, 109 –110.

Lu, T., Chen, F., (2012). Quantitative analysis of molecular surface based on improved Marching Tetrahedra algorithm, J. Mol. Graph. Model (38): 314-323

Martin, F., Zipse, H., (2005). Charge distribution in the water molecule--a comparison of methods. J Comp Chem. (26): 97 – 105

Monajjemi, M., Lee, VS., Khaleghian, M., Honarparvar, B., Mollaamin, F., (2010). Theoretical Description of Electromagnetic Nonbonded Interactions of Radical, Cationic, and Anionic NH2BHNBHNH2 Inside of the B18N18 Nano ring. J. Phys. Chem. C (114) 15315

Monajjemi, M., Khaleghian, M., (2011). EPR Study of Electronic Structure of [CoF6] and B18N18 Nano Ring Field Effects on Octahedral Complex. J Clust Sci (22):673–692 DOI 10.1007/s10876-011-0414-2

Monajjemi, M. (2012). Quantum investigation of non-bonded interaction between the B15N15 ring and BH2NBH2 (radical, cation, anion) systems: a nano molecular motor, *Struct. Chem*. (23): 551

Nishinaga, T., Ohmae, T., Iyoda, M. (2010). Recent Studies on the Aromaticity and Antiaromaticity of Planar Cyclooctatetraene. Symmetry 2, 76–97.

Naor, R., Luz, Z., (1982). Bond Shift Kinetics in Cyclo -Octatetraene by Dynamic NMR in Liquid Crystalline Solvents. The Journal of Chemical Physics 76, 5662–5664.

Perdew, J. P., Burke, K., Ernzerhof (1996). Generalized Gradient Approximation Made Simple. Phys. Rev. Lett. (77): 3865-3868

Schild, A., Paulus ,B., (2013). Multireference calculations for ring inversion and double bond shifting in cyclooctatetraene. J Comput Chem 34:1393–1397.

Stevenson, C.D., Brown, E.C., Hrovat, D.A, Borden, W.T (1998). Isotope effects on the ring inversion of cyclooctatetraene. J Am Chem Soc 120:8864–8867.

Streitwieser, A. Jr. (1961). Molecular Orbital Theory for Organic Chemists, Wiley, New York, 1; b) N. C. Baird, M. A. Whitehead, Can. J. Chem. 1966, 44, 1933 –1943.

Wenthold, P.G., Hrovat, D.A., Borden, W.T., Lineberger, W.C. (1996). Transition-state spectroscopy of cyclooctatetraene. Science 272:1456–1459.

Yoshida, T., Tokizaki, C., Takayanagi, T., (2015). Theoretical Analysis of the Transition-State Spectrum of the Cyclooctatetraene Unimolecular Reaction: Three Degree-of Freedom Model Calculations. Chem. Phys. Lett., 634, 134–139.

Willstätter, R., Waser, E (1911). "Über Cyclo-octatetraen" [On cyclooctatetraene]. Ber. Dtsch. Chem. Ges.44 (3): 3423–3445. doi:10.1002/cber.191104403216.

Willstätter, R., Heidelberger, M., (1913). Zur Kenntnis Des Cyclo-Octatetraens. Chem. Ber. 46, 517–527.

Wu, J. I., Fernández, I., Mo, Y., Schleyer, P. V. R. (2012). Why Cyclooctatetraene Is Highly Stabilized: the Importance of "Two-Way" (Double) Hyperconjugation. J. Chem. Theory Comput. 8, 1280–1287.